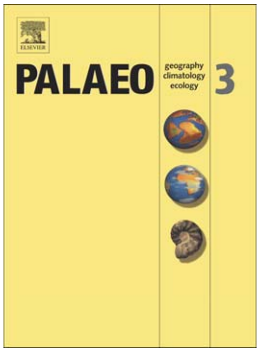

Quaternary dust source variation across the Chinese Loess Plateau

Anna Bird, Thomas Stevens, Martin Rittner, Pieter Vermeesch, Andrew Carter, Sergio Andò, Eduardo Garzanti, Huayu Lu, Junsheng Nie, Lin Zeng, Hanzhi Zhang, Zhiwei Xu

PII: S0031-0182(15)00321-1
DOI: doi: 10.1016/j.palaeo.2015.06.024
Reference: PALAEO 7325

To appear in: *Palaeogeography, Palaeoclimatology, Palaeoecology*

Received date: 22 February 2015
Revised date: 29 May 2015
Accepted date: 19 June 2015

Please cite this article as: Bird, Anna, Stevens, Thomas, Rittner, Martin, Vermeesch, Pieter, Carter, Andrew, Andò, Sergio, Garzanti, Eduardo, Lu, Huayu, Nie, Junsheng, Zeng, Lin, Zhang, Hanzhi, Xu, Zhiwei, Quaternary dust source variation across the Chinese Loess Plateau, *Palaeogeography, Palaeoclimatology, Palaeoecology* (2015), doi: 10.1016/j.palaeo.2015.06.024

Quaternary dust source variation across the Chinese Loess Plateau

Anna Bird[1,2], Thomas Stevens[1,3], Martin Rittner[4], Pieter Vermeesch[4], Andrew Carter[4, 5], Sergio Andò[6], Eduardo Garzanti[6], Huayu Lu[7], Junsheng Nie[8], Lin Zeng[7], Hanzhi Zhang[7], Zhiwei Xu[7]

[1]Department of Geography, Royal Holloway University of London, Egham, Surrey, TW20 OEX, UK

[2]Current address: Department of Geography, Environment and Earth Sciences, University of Hull, Hull, HU6 7RX, UK. a.bird@hull.ac.uk

[3]Current address: Department of Earth Sciences, Villavägen 16, Uppsala University, Uppsala, 75236, Sweden

[4]London Geochronology Centre, Department of Earth Sciences, University College London (UCL), London, WC1E 6BT, UK

[5]School of Earth Sciences, Birkbeck College, University of London, London, WC1E 7HX, UK

[6]Dipartimento di Scienze Geologiche e Geotecnologie, Università di Milano-Bicocca, Piazza della Scienza 4, 20126 Milano, Italy

[7]School of Geographic and Oceanographic Sciences, Institute for Climate and Global Change Research, Nanjing University, Nanjing 210093, China

[8]Key Laboratory of Western China's Environment System, Ministry of Education, Lanzhou University, Lanzhou, Gansu 730000, China

ABSTRACT

The Chinese Loess Plateau in north central China contains one of the most valuable Cenozoic climate archives on land. Establishing the origin of this substantial archive of aeolian sediments is critical for the interpretation of loess climate proxies, past atmospheric wind patterns and changing climatic/tectonic controls on erosion over potentially the past 25 Ma. Despite this significance there are a number of disagreements over the precise source areas and the extent to which these vary through time and across the plateau. To address this, we utilize a multi-technique, approach of combined detrital single-grain zircon U-Pb dating and heavy mineral analysis to establish the sources of loess through the Quaternary and constrain their variation geographically across the Loess Plateau. We combine our data with suitable published single-grain datasets from loess and possible source regions. The results demonstrate a dramatic spatial heterogeneity of dust sources across the plateau. Sites to the west of the Loess Plateau show strong affinity to the Yellow River and the northern Tibetan Plateau, while further east the influence of North-China-Craton-derived material becomes more significant (Fig. 1). This spatial variability in source implies a far more complex relationship to dust sources than previously envisioned. The provenance of loess/soil units also varies through time, although there is no consistent relationship between these shifts and changing glacial/interglacial periods, as hypothesized previously. This variation demonstrates highly dynamic and variable dust sources and transport modes that are influenced by to abrupt climate shifts within individual glacial-interglacial episodes, and potentially to the dynamics of the Yellow River system.

INTRODUCTION

The Chinese Loess Plateau in north-central China (Fig. 1) covers an area of ~360,000 km^2 (Li & Lu 2010) and potentially contains ~25 Ma of loess accumulation (Qiang et al., 2011), the longest and most continuous dust archive on the planet (Liu and Ding, 1998; Guo et al., 2002). These sequences comprise alternating Quaternary loess and soil layers, underlain by finer-grained Pliocene-Miocene Red Clay and Miocene-Eocene loess. A number of sandy deserts and mountain belts lie to the north and northwest of the Loess Plateau and may act as dust sources to the area (e.g. Honda et al., 2004; Liu et al., 2004; Sun et al., 2002; Pye & Zhou, 1989; Clarke 1995; Maher et al., 2009; Guan et al., 2008), while Cretaceous sandstone underlies the majority of the Loess Plateau and the semi-arid Mu Us Desert to the north (Fig. 1).

Dust accumulation on the Loess Plateau is a consequence of winter monsoon near-surface winds generated by the Siberian high-pressure system and/or westerly driven spring dust storms (Porter, 2001; Roe, 2009). This regime allows for a large number of potential dust source regions, ranging from west to north of the plateau, and encompassing a wide range of high-mountain, piedmont, fluvial, playa, sandy and Gobi desert environments that have the potential to emit dust (Honda et al., 2004; Liu et al., 2004; Sun et al., 2002; Pye & Zhou 1989; Clarke 1995; Maher et al., 2009; Guan et al., 2008). This is of considerable importance to resolve as loess deposits are regarded as one of the most important records of climatic change on land (Ding et al., 2002) yet ambiguity over dust sources limits the extent to which climate changes can be inferred from proxy data (Stevens et al., 2013a).

Previous work using grain-size, geochemical and mineralogical data suggest various possible dust origins via desert processes in NW China (Honda et al., 2004; Liu et al., 2004) and Mongolia (Sun et al., 2002; Pye & Zhou 1989), or via mountain processes in Tibet, Qilian or Gobi Altai (Clarke 1995; Maher et al., 2009; Guan et al., 2008). Much of this previous work used bulk sediments or whole-rock samples to track sources (e.g. Sun et al., 2000; Ding et al., 2002; Gallet et al., 1996). While these methods can still provide valuable insights into source via analysis of potential mixing lines in data (Zhao et al., 2014), they have the disadvantage of averaging out multiple distinct sediment source signatures. As such, more recent studies have used single-grain approaches such as detrital zircon U-Pb geochronology on Chinese Plateau Loess (Stevens et al., 2010, 2013b; Pullen et al., 2011; Che & Li 2013; Xiao et al., 2012; Nie et al., 2014) and loess deposits elsewhere (e.g. Aleinkoff et al., 1999) in order to distinguish the potential influence of multiple dust sources. A disadvantage of analyzing single-grains in silt-sized material in all of these studies (Aleinkoff et al., 1999; Stevens et al., 2010, 2013b; Pullen et al., 2011; Che & Li 2013; Xiao et al., 2012; Nie et al., 2014) is that the size of the laser spot is c. 35 µm, limiting analyses to grains over 40 µm. This biases the dataset towards coarser material, and therefore probably more proximal sites, although such near source studies are still an important aspect of dust sourcing (Formenti et al., 2011). Another important point to take into consideration is grain-size variation across the Chinese Loess Plateau; northern sites show higher coarse silt and sand content than the more clay enriched southern sites (Yang and Ding, 2008). This change in grain-size also corresponds to a change in mineralogy, with northern sites richer in feldspar and hornblende and southern sites richer in micas and poorer in heavy minerals, especially unstable types (Eden et al., 1994). This decrease in heavy minerals contents is also seen down-section at Luochuan (Nie et al., 2013). However, this variation across the Plateau will cause a bias in all provenance techniques (e.g. bulk isotopes, Ar-Ar in micas and hornblende, Pb isotopes in feldspars), not just detrital zircon U-Pb. Despite these limitations this new single-grain work has greatly refined understanding of dust sources to the Loess Plateau, although a number of debates and uncertainties remain. While many of these studies generally emphasize direct aeolian transport from a northeastern Tibetan Plateau source, Che and Li (2013) suggest an additional source input from the Gobi Altai Mountains via the Alxa arid region (including the Baidan Jaran and Tengger deserts; Fig. 1). Furthermore, Stevens et al. (2013b) highlight the potential role of the Yellow River in transport of dust and sand from the NE Tibetan source regions to the Loess Plateau and western Mu Us desert, immediately to the north (Fig. 1).

Previous bulk sediment studies have also been split over whether dust sources to the Loess Plateau evolved through the Quaternary (Sun, 2005) and varied between glacial and interglacial periods (Sun et al., 2008), or were uniform through time (Chen et al., 2007; Gallet et al., 1996; Wang et al., 2007). A single-grain study has also suggested that there may be source variation between glacial and interglacial periods due to shifts in westerly storm tracks between these periods, with glacial-age loess sourced from the Qaidam Basin and interglacial dust sourced from further north (Xiao et al., 2012). Other authors argue that any variation is an artifact of sampling and analytical procedures, and when that is accounted for, no variation between sampled loess and soil units can be seen (Che and Li, 2013). In contrast, heavy mineral, bulk geochemical and quartz luminescence data demonstrate an abrupt millennial scale source shift within the last glacial loess unit L1 from Beiguoyuan on the northwest Loess

Plateau (Stevens et al., 2013a), Finally, there is also uncertainty over whether sources shift from the Pliocene Red Clay to Quaternary loess (Sun & Zhu, 2010; Nie et al., 2013; 2014).

Furthermore, while many bulk sediment studies have often assumed that loess sources are similar across the Loess Plateau, single-grain studies have provided conflicting evidence over whether dust sources vary spatially. Xiao et al. (2012) argue that their zircon U-Pb data demonstrate changing sources across the plateau. However, Che and Li (2013) also explain such variation through sampling uncertainties. As yet insufficient single-grain data have been published to fully evaluate whether sources shift across the region, despite the clear importance for understanding dust transport pathways.

A clear way forward is specified by Nie et al. (2012), who advocate an integrated, multi-technique approach as best for provenance studies where issues such as recycling, non-unique sources, and pre- and post-depositional modifications may complicate interpretation of results based solely on individual provenance techniques. A multi-proxy approach also allows some consideration of the potential hydraulic effects on particle size and mineral type along a transport pathway by focusing on minerals that have different densities and that can be analyzed at different grain sizes. Furthermore, part of the difficulty in addressing the debates above still comes from a paucity of data, which limit the statistical validity of provenance interpretations (Che and Li, 2013). While the exact number of grains needed in a provenance study is debated (Vermeesch, 2004; Che and Li, 2013; Sláma and Košler, 2012), the number of analyzed sections required to demonstrate varying or constant provenance in time and space is not yet sufficient. Thus, a larger-scale, systematic study using multiple provenancing techniques is needed to resolve the questions over loess provenance through time and across the Loess Plateau. Here we go beyond previous work by applying a multi-proxy, single-grain approach of combined zircon U-Pb and heavy mineral analyses using novel statistical approaches on a larger set of samples from more Quaternary loess/soil sections and individual units than in previous studies. Heavy mineral analysis is a useful technique to complement zircon U-Pb as only a small amount of sample is needed and it allows the effects of weathering and potential hydraulic sorting to be examined. We also incorporate existing loess and source region U-Pb and heavy mineral data to enhance the dataset as much as possible. Here we focus on the Quaternary source variation within the loess-palaeosol sequences.

SAMPLES AND METHODS

Approximately 3 kg samples were taken from each sampling point in the Luochuan, Jingbian, Beiguoyuan and Lingtai loess sections (summarized in Table 1; locations Fig. 1). A Cretaceous sandstone sample (CH11-MU-01) was also taken from the north-western edge of the Loess Plateau to compare to existing results from the wider area underlying the Mu Us Desert (Stevens et al., 2013b). Specific loess/soil units for the analyzed samples are assigned using stratigraphic nomenclature from Ding et al. (2005) for Jingbian, Sun and Liu (2000) for Luochuan, and Ding et al. (1999) for Lingtai. The youngest part of the succession is the Holocene soil S0, the underlying loess unit L1 (Malan Formation), and the underlying soil unit S1, etc. The Lishi Formation then comprises the period from the last interglacial to the early Mid-Pleistocene (S1 to L15) and the Wucheng loess formation continuing to the base of the Pleistocene (L34) (~2.8 Ma; Yang & Ding, 2010).

The methods follow Stevens et al. (2013b). Heavy mineral separation for zircon U-Pb analysis took place at the NERC Isotope Geosciences Laboratory (NIGL) and University College London (UCL). The zircon U-Pb analyses took place at UCL/Birkbeck College London following the methods of Jackson et al. (2004), using a New Wave aperture-imaged frequency quintupled UP213 laser ablation system (213 nm) coupled to an Agilent 7700 quadruple inductively coupled plasma mass spectrometer (ICP-MS). Analyses were run with a laser spot diameter of 35 µm, 10 Hz pulse repetition rate and an energy fluence of ~2.5 J cm^{-2}. Data reduction was conducted with Glitter (Griffen et al., 2008) and calculations followed Ludwig (1999). Data concordant to +10/-15% were included and the cut off for changing from ^{206}Pb/^{238}U to

^{207}Pb/^{206}Pb age was at 1100 Ma. All zircon U-Pb data are in Supplementary File 1, including number of grains analyzed per sample, and the number that were concordant. All detrital age spectra are presented as Kernel Density Estimates (KDE) (Vermeesch, 2012).

Mineral separations for heavy mineral analysis took place at Royal Holloway and at the University of Milano-Bicocca. Methods for heavy mineral separation followed Mange & Maurer (1991). Samples were either wet sieved through 250 µm, 63 µm and 40 µm meshes, then through only 250 µm and 40 µm meshes to increase efficiency. Density separation was undertaken using sodium polytungstate (density 2.89 cm^3) with heavy mineral fractions mounted on glass slides with Canada balsam for analysis under a petrographic microscope. At the University of Milano-Bicocca at least 200 transparent heavy minerals were determined for each sample by the “area” method of grain counting. At Royal Holloway at least 300 transparent heavy minerals were counted. Replicate counts were made at both institutions to assess counting differences, with a maximum difference of 1% (Supplementary file 2).

The very large dataset presented within this paper adds to a substantial existing Cenozoic sediment single-grain provenance dataset, covering northern and northwest China (Lease et al., 2007, 2012; Enkelmann et al., 2007; Xie et al., 2007; Stevens et al., 2010, 2013b; Pullen et al., 2011; Xiao et al., 2012; Che & Li, 2013). In order to compare these datasets effectively and visualize (dis-) similarities, multidimensional scaling (MDS) maps (Vermeesch, 2013) are used on zircon and heavy mineral data, once the heavy mineral data have been converted to logratio-normalised data, following Aitchinson (1986). All MDS maps are plotted with their corresponding Shepard plots, allowing a graphical evaluation of the quality of the MDS model fit by plotting the calculated MDS map distance between two points against the corresponding calculated dissimilarity. The “stress parameter” (Kruskal, 1964) quantifies the goodness-of-fit of the MDS map compared to the calculated dissimilarity. Stress values up to ~10% are usually deemed acceptable. Detailed description of this method is found in Vermeesch

(2013). The method has been used to successfully show differences in Mu Us sand sources in different parts of the desert by Stevens et al. (2013b).

RESULTS

Zircon U-Pb ages

Zircon U-Pb ages were obtained from samples from Beiguoyuan, Jingbian and Lingtai. The zircon U-Pb age KDEs from all the loess and soil samples (Fig. 1) show two dominant peaks at 260-290 Ma and at 440-480 Ma (Fig. 2). The 440-480 Ma peak is dominant in all Beiguoyuan and Lingtai samples apart from CH11-05-04 and CH11-05-06, from L1LL1 and L1LL2 respectively, where the magnitude of the peaks are similar. All samples also show a spread of Precambrian ages, with some showing very diffuse and largely indistinct peaks centered around 1 Ga, 1.9 Ga and 2.5 Ga. Jingbian, a desert marginal site to the northeast of the Loess Plateau, shows two main differences compared to Lingtai and Beiguoyuan. First, the 260-290 Ma peak is dominant in all samples apart from those from the early Quaternary Wucheng succession (CH11-04-10 and CH11-04-11), where the peak is approximately equal with the peak at 440-480 Ma. Second, the Pre-Cambrian ages are more dominant than at other sections, although the small diffuse cluster at 2.5 Ga is similar to those from Beiguoyuan and Lingtai. Sample CH11-MU-01 from the Cretaceous sandstone has KDE peaks at 260-290 Ma, 1.9 Ga and 2.5 Ga and no 440-480 Ma peak, and is similar to other Cretaceous sandstone samples further to the east and north presented in Stevens et al. (2013b). The samples from Lingtai and Beiguoyuan yield zircon U-Pb data that are almost identical to the last glacial maximum sample from Stevens et al. (2010), also from Beiguoyuan. The distributions are also very similar to samples from the western part of the Mu Us desert, as well as a sample from the Yellow River (YR1) upstream of Lanzhou to the west of the Loess Plateau (Fig. 2; Stevens et al., 2013b). The MDS plot for the samples analyzed within this study (Fig. 3) shows that Jingbian sediments consistently plot in a different area from Beiguoyuan and Lingtai, (highlighted in the circle number 1 in Fig. 3). For example, samples from L3 from Jingbian show a dominant 260-290 Ma peak while at Beiguoyuan there is a dominant 440-480 Ma peak.

Heavy mineral analysis

Sixteen samples from all four loess sections were analyzed for their heavy mineral assemblage, including analysis of weathering and diagenetic effects on the individual mineral grains (Andò et al., 2012). Most of the samples show similar heavy mineral assemblages, dominated by epidote and amphiboles with pyroxene, apatite, rutile and garnet. Rarer monazite, chloritoid, kyanite, andalusite and sillimanite are found in some samples (Fig. 4). The zircon, tourmaline and rutile fraction is mostly unweathered; there are also some unweathered amphiboles and epidotes but most are corroded with some etched grains (Andó et al., 2012). Pyroxenes are the most weathered with the majority of grains being corroded or etched. Around 50% of garnet is unweathered. The most weathering is seen in the samples from the Cretaceous sandstone and the Red Clay samples from Luochuan, on the central Loess Plateau, and Lingtai. The least weathered samples are from Beiguoyuan loess.

The heavy mineral assemblages from the analyzed samples suggest an orogenic source (Philip, 1968; Garzanti & Andò, 2007a; Garzanti et al., 2007), with common diopsidic to augitic clinopyroxene indicating additional mafic (gabbro, andesite/basalt, or even calcsilicate) sources. The presence of hornblende, actinolite and glaucophane suggest provenance from a range of metamorphic rocks, including blueschist, greenschist and amphibolite facies. This is confirmed by the presence of epidote, garnet, staurolite and a few aluminosilicates, which also suggest at least some of the source rocks are pelitic in composition. The samples from the Cretaceous sandstone and the Red Clay are dominated by garnet and epidote and less amphibole than the loess samples. This suggests that these sample have been more affected by diagenesis than the latter, but are still recording an orogenic source (Fig. 4;

Morton and Hallsworth 2007). Notably, the amphibole glaucophane is found especially in Beiguoyuan and Lingtai. Glaucophane is only found in high pressure, low temperature rocks, typically blueschists, which need slow heating and extremely rapid uplift in order to be preserved, usually formed during subduction processes (Deer et al., 1992). Blueschists are only commonly found in three places in China, west Junggar, west Tien Shan and northern Qilian (Liou et al., 1989).

The heavy mineral MDS plot shows some discrete groupings (Fig. 5). The Cretaceous sandstone samples and the eastern Mu Us samples plot in separate areas from the loess (Fig. 5, circle 2), as does the Lingtai Red Clay sample (CH11-06-15). In contrast, the loess, soil, Red Clay, Yellow River and western Mu Us desert samples all plot much closer together. However there are some clusters, with Jingbian plotting closest to the western Mu Us samples (Fig.5, circle 3), and also overlapping with some of the western Mu Us samples. Luochuan samples plot separately from Lingtai and Beiguoyuan (Fig. 5, circle 1) and one sample (CH04-01-30) from Beiguoyuan, highlighted in a square in Fig. 5, is distinct from the rest of the samples from the same section.

DISCUSSION: TESTING PREVIOUS HYPOTHESES

Major dust source to the Chinese Loess Plateau

The new and previously published zircon U-Pb data show that the Quaternary loess is not solely sourced from the Qaidam Basin, the Cretaceous sandstone, the Tengger Desert, the Eastern Mu Us, the samples from the deserts in north eastern China, Central Mongolia, Parmir or sample YG02 from the Gobi Altay mountains (Che and Li, 2013) (Fig. 7). The loess is most similar to sediments from the Yellow River, western Mu Us desert, the Tarim Basin, Xining and sample RSH01 (Figs1, 6 and 7, circle 2; Lease et al., 2007, 2012; Enkelmann et al., 2007; Xie et al., 2007; Stevens et al., 2010; Pullen et al., 2011; Xiao et al. 2012; Che & Li, 2013; Stevens et al., 2013b). Individual terranes from the northern Tibetan Plateau show some similarities with the loess samples but also some differences. For example, while loess samples show peaks at c. 280 and 450 Ma, samples from western Kunlun Mountains (Pullen et al., 2011; Bershaw et al., 2012) only show a peak at c. 450 Ma. By contrast, Qaidam sediments (Lease et al., 2007; 2012) show both peaks but also has an additional peak at ~50 Ma peak. However, if the Yellow River sample is taken as an integrated sample of the various northern and northeastern Tibetan terranes of its drainage area (which is often the case for large river systems and their catchments (Lease et al., 2007)), then the combined northern Tibetan signatures as represented in that sample are very similar to the loess samples. A northeastern Tibetan source interpretation for the Chinese Loess Plateau is consistent with zircon U-Pb results from Stevens et al. (2010; 2013b), Pullen et al. (2011) and Xiao et al. (2012). However, two other possibilities are; dust origins in the Tarim basin and the Che and Li (2013) suggestion of binary loess sources from the Northern Tibetan Plateau and the Gobi Altay Mountains, mixing together in the Alxa sandy lands north of the Tibetan Plateau. However, below we argue that the data are most consistent with a NE Tibetan source.

The MDS map used by Che and Li (2013; Fig. 3) to argue for mixed sources shares many similarities with our Fig. 7, in spite of the different method of obtaining pairwise distances between points. However, there are also some significant differences. Notably, the data from the Gobi Altay Mountains plot in a separate area on their MDS map than do the loess samples in this study (Fig. 7). This difference may be partly due to the different datasets used in construction of the map. The map shows distance (dissimilarity) between samples and as soon as any new data points are added it will have a slightly different configuration. With our new data and comprehensive analysis of published data, the age spectra from the Gobi Altay sample is not an obvious loess source candidate, although some input from this area cannot be completely ruled out as only one sample from that area has been analyzed (YG01, Fig.1, 6, 7). Furthermore, the sample (RSH01, Fig. 1) used by Che and Li (2013) to represent the Alxa Arid

Lands is sediment from a river that drains the Qilian Mountains, and is therefore comprised dominantly of part of the assemblage of terranes that make up northern Tibet. Indeed, this sample lies close to the loess on the MDS map, reinforcing the hypothesis that the main source for the Chinese Loess Plateau is the northern Tibetan Plateau, rather than the Alxa region. Finally, the presence of glaucophane especially in Beiguoyuan and Lingtai samples suggests that the Gobi Altay is not a major source as it is not one of the main glaucophane-rich areas in the region. Glaucophane can be found in Qilian on the northern Tibetan Plateau, and the Tien Shan and Junggar in the west of China. Qilian in particular may be the most probable source due to its proximity to the Loess Plateau, as the glaucophane is relatively uncorroded or etched (Andò et al., 2012). Nonetheless, the possibility of binary sources is an intriguing concept that requires further analysis of more samples from the Gobi Altay Mountains and Alxa Arid Lands.

The Tarim Basin shows similar zircon U-Pb age distributions when compared to the loess, although this is based only on one sample (Xie et al., 2007; Figs 6 and 7). While more analyses of the Tarim Basin sediments are needed, we suggest that this is an unlikely source for a number of reasons. First, the required dust transport pathways from Tarim to the Loess Plateau cross a number of the sampled desert areas (Fig. 1). This would imply that all the deserts and sediment areas along this transport pathway should show a similar zircon U-Pb age distribution to the Tarim Basin and the Loess Plateau, or some clear trend line, if fluvial inputs of new and distinct source signatures from adjacent mountains were more significant than input from aeolian transport. However, as has been discussed above, no similarity or clear trend is seen in the Alxa (Che and Li, 2013) and Tengger Desert samples (Stevens et al., 2010), the latter only showing one U-Pb age peak at <500 Ma at ~280 Ma, typical of the North China Craton, and the former showing a different, more diffuse, younger peak than the Tarim sample (Fig. 6). Also, dust from an ice core near Qaidam and the Hexi Corridor (Fig. 1) has a geochemical signature similar to dust from the Tarim Basin, but different from the Chinese Loess Plateau (Wu et al., 2009), again suggesting dust is not transported all the way along the Hexi Corridor to the Loess Plateau. Second, the heavy minerals from the loess samples are relatively pristine with the presence of unstable species like pyroxene and amphibole. If these sediments were to travel ~2000 km from the Tarim Basin to the Loess Plateau, it would be expected that the unstable minerals would be very rounded, etched and corroded, with no euhedral and few pristine minerals left. Long-distance Aeolian transport would likely involve phases of deposition and deflation with episodes of sediment weathering. Thus, the lack of heavily etched or corroded unstable minerals in the loess samples suggests this did not occur. Furthermore, the presence of relative pristine, euhedral to sub-rounded glaucophane especially in the Beiguoyuan and Lingtai samples reinforces the probability of a more proximal high-pressure belt to the Loess Plateau acting as source, like Qilian on the northeastern Tibetan Plateau. Finally, it has been noted previously that direct coarse dust transport from the Tarim basin to the Loess Plateau would be greatly limited by the high topographic barriers surrounding the basin and the area’s prevailing wind patterns (Sun, 2002). Given the dominant medium to coarse silt composition of loess it remains unlikely that such a distal source as the Tarim basin would contribute sufficient coarse grains transported for distances exceeding 2000 km (Fig. 1).

Thus, given the combined evidence and a process of elimination, the most likely explanation of the provenance data is that the majority of the sediment on the Chinese Loess Plateau is transported there from north-eastern Tibetan Plateau. Whether this involves some role for the Yellow River in sediment routing before final aeolian transport requires further testing, but the coarse particle sizes of material transported from NE Tibet to the western Mu Us Desert and Loess Plateau makes this a clear possibility.

Source variation across the Chinese Loess Plateau

While the dominant characteristics of the Loess Plateau zircon U-Pb data suggest north-eastern Tibetan Plateau sources, there is variation across the Loess Plateau that tends to be most pronounced in the U-Pb data of Jingbian and the heavy mineral data at Luochuan (Figs 5 and 7). The U-Pb age spectra from Jingbian share most of the same features with the other loess sites, the Yellow River and the western Mu Us desert (Fig. 7), suggesting NE Tibet is still a major source. However, the relatively more dominant 260-290 Ma peak, present in all samples from Jingbian, suggests a greater input from other sources that match samples from the Quaternary-modern eastern Mu Us Desert and the underlying Cretaceous sandstone (Fig. 7; Stevens et al., 2013b). This suggests that at this coarse-grained and desert marginal site on the north-east of the Loess Plateau, the underlying and locally derived North China Craton material is of increased importance. While a north-eastern Tibetan Plateau signal dominates source signatures over the majority of the Loess Plateau, Jingbian therefore does show some evidence of a mixture of North China Craton and Tibetan sources, similar to the suggestion by Che and Li (2013), although more likely related to the directly neighboring Mu Us.

When comparing heavy mineral assemblages down section between the study sites, Jingbian exhibits the least down-section variability when compared with the other sites. While this may be related to source differences highlighted by the U-Pb data, this is more likely because Jingbian experienced the driest environment of the sample sites, on the margin of the semi-arid Mu Us. This along with the high sedimentation rates at the site reduces diagenesis, leaching and weathering. In contrast, Luochuan's heavy mineral assemblages show an increase in epidote and a decrease in amphibole down section, and almost no pyroxene. This shows that Luochuan has been more influenced by weathering/diagenesis than the other sections, possibly due to a wetter, more humid climate (Nie et al., 2013). However, the heavy mineral assemblages at Lingtai are much less weathered than those at Luochuan, even though the latter is only situated c. 190 km east and at present shares a similar climate. This could potentially imply that Luochuan had a wetter climate than Lingtai in the past but there is little stratigraphic evidence of this. Although speculative, a more parsimonious explanation could be that, given the dominance of dust sources located to the west on the NE Tibetan plateau, sediment that reaches Luochuan may have been reworked within the Loess Plateau or weathered more en route than loess preserved at the more western Lingtai site, suggesting west-east dust transport within the Loess Plateau, which has also been demonstrated in other studies on past and present dust transport (Roe, 2009; Pullen et al., 2011). The presence of more unweathered glaucophane at the northern and western Beiguoyuan and Lingtai sites reinforces this possibility.

Given the differences in source suggested between sites reported here, and also within the study of Xiao et al. (2012), we consider on why such differences were not seen by Che and Li (2013) using their zircon U-Pb data. Che and Li (2013) suggested that the reason for the discrepancies between their findings and those of Xiao et al. (2012) were dominantly due to the effect of small sample sizes in the latter study. However, it has recently been argued by Sláma and Košler (2012) that only 60 analyses per sample are sufficient for a reproducible age spectrum and that increasing the number of analyses to >100 grains does not result in significantly improved reproducibility. Under this scenario the between sample differences seen in the Xiao et al. (2012) data are likely valid representations of real provenance differences in the population. Irrespective, many of the individual sample analyses presented here include grain counts greater than the 100 grain cut off proposed by Che and Li (2013), yet there is evidence for between site variation. Indeed, the 95% variation envelope shown for all zircon U-Pb ages in Che and Li (2013) (including data from Pullen et al. (2011); Xiao et al. (2012) and Stevens et al. (2013b)) using Monte Carlo simulation cannot be used to test for differences or similarities between individual samples within the same dataset, as this envelope may in fact simply be representative of real source variation within that sample set. Furthermore, similar variation between sites is also seen in the heavy mineral data (Fig. 4). Despite these issues, and the differences between studies, Che and Li (2013) raise an extremely valid question over the range of statistical variation seen within loess samples coming from a single source population. As this has not been defined properly, estimating significant differences indicative of source differences between datasets is difficult. One alternative explanation for the differences between the studies also comes from Sláma and Košler (2012): differences in sample preparation and grain analysis techniques between studies, which may introduce a bias effect. This is a challenge for the provenance community in general as a uniform set of parameters for detrital zircon U-Pb handling and analysis methods are needed.

Source shifts through time

In addition to geographical variation, recent zircon U-Pb work on the Chinese Loess Plateau has resulted in conflicting hypotheses over whether dust sources shift through time, notably between glacial and interglacial periods (Xiao et al., 2012; Che and Li, 2013). Nie et al. (2014) used zircon U-Pb data to argue for long term shifts in Pliocene to Quaternary dust sources, although here we restrict our analysis to changes within and between glacial and interglacial units of the Quaternary. Our combined heavy mineral and zircon U-Pb results here do not show a consistent pattern of glacial/interglacial source shifts at individual sites (Figs 3 and 5), as suggested by Xiao et al. (2012). Changes in heavy mineral assemblage through time can be explained almost entirely by weathering (Figs 4 and 5) and there is no consistent pattern between units in the zircon data, despite some variation in age spectra (Figs 2 and 3).

This lack of consistent pattern fits with the Che and Li (2013) interpretation of their data. This implies that the atmospheric transport pathways during glacial and interglacial periods do not vary sufficiently for a source change, or that shifting transport pathways still pass over identical source rocks.

Alternatively, this evidence would also fit with the hypothesis of the Yellow River being the main source of loess to the Loess Plateau (Stevens et al., 2013b).

However, previous work indicates that during the last glacial, a substantial and abrupt shift in source at Beiguoyuan is shown in heavy mineral, bulk geochemical and quartz luminescence characteristics, broadly coincident with Heinrich event 2 (Stevens et al., 2013a). In fact, the one sample from Beiguoyuan (CH04-01-30) that plots away from the main Beiguoyuan group here (Fig. 5) was analyzed by Stevens et al. (2013a) and was taken from part of the 2 m thick unit that shows these different source characteristics. This finding, combined with the generally inconsistent variability between provenance data in samples here, implies that abrupt changes in dust sources can occur during individual glacial and interglacial phases, and that these are at least as significant as any source shifts between glacial-interglacials. Indeed, there is considerable evidence for dramatic variation in monsoon intensity and westerly storm track position within individual glacial and interglacial phases from various northern hemisphere records (Wang et al., 2001; Wang et al., 2005; Eynaud et al., 2009). This variability suggests that the provenance signature of a sample from a single loess or soil unit will be heavily dependent on whether it falls within a stadial or interstadial phase, and on the applied sampling interval. The coarse sampling resolution of single-grain geochronological analyses, necessitated by the number of grains needed to make analyses statistically meaningful and the labor-intensive techniques involved, may not therefore be detailed enough to separate patterns in intra- and inter-unit variability in provenance studies. In other words, despite there being variation in zircon U-Pb age spectra down individual sections, no clear pattern emerges as source variation within individual glacial or interglacial stages may be at least as significant as provenance changes between these stages. Currently there is no sufficiently highly stratigraphically resolved single-grain data to identify these trends. Future work should focus on detailed sampling to reveal whether the abrupt within unit provenance shifts seen at Beiguoyuan (Stevens et al., 2013a) are more widespread and how this compares to between-unit variability.

Implications for dust generation and transport

Dust deposition rate on the Loess Plateau is often considered a function of wind-speed and source aridity, and is used extensively as a climate proxy indicator (Porter, 2001). However, potential abrupt changes in source undermine this and differences in source across the Loess Plateau further complicate this picture, making the use of sedimentological characteristics such as grain-size and accumulation rate as climate proxies difficult. Furthermore, if dust is delivered from the northeastern Tibetan Plateau to the majority of the Loess Plateau via the Yellow River, as hypothesized by Stevens et al. (2013b) and as is consistent with data presented here, then variations in accumulation rates will be a function of a number of other factors; notably denudation of the Tibetan Plateau, river dynamics and sediment availability. Increased uplift or climate driven erosion and rates of river incision will increase the amount of sediment carried in the Yellow River, which could lead to increased loess mass accumulation rates over tectonic or glacial-interglacial timescales. Sediment availability would also be impacted by the fluvial hydrology of the upper and middle reaches of the Yellow River, with incision and aggradation as well as deposition and activation of flood plains as controlling factors, themselves influenced by changing climate and base level. While it is clear that loess mass accumulation rates increase during glacial phases (Kohfeld and Harrison, 2003) and climate influences dust production and deposition, the possibility of Yellow River dynamics influencing loess deposition requires further analysis in order to properly understand the implications for understanding climate proxy records and past atmospheric dust transport records from loess. Of particular importance to these issues are the questions: how old is the Yellow River and when did it start to follow its current course? What are the provenance signatures of the river through time and along its course? Is it possible to relate variations within the loess accumulation to changes in the Yellow River? Are the changes in provenance shown within individual sites a function of river dynamics or changing aeolian dust sources? These questions will require extensive future analysis of loess and Yellow River sediments but will shed light on the tectonic and climatic controls on one of the most important dust and terrestrial climate archives on the planet.

CONCLUSIONS

Analysis of single-grain zircon U-Pb age and heavy mineral assemblages from loess samples across the Chinese Loess Plateau indicate that there is geographical and temporal variation in sediment source. Our data show that while the majority of Quaternary loess sites show a close affinity to the Yellow River and northern Tibetan Plateau sources, at Jingbian on the northeastern Loess Plateau margin the provenance signatures show some similarity to northern deserts and North China Craton material. Our results show some possible variation between age spectra down individual loess sections, but no systematic source variation between loess and soil units, implying that short-term fluctuations in source are at least as important as any glacial interglacial changes. The most striking down section variation is recorded by the heavy minerals and relates to increased diagenesis/weathering. The spatial and temporal variability in source demonstrated from the data implies a far more complex relationship of deposited loess to dust sources than previously envisioned. Finally, the results here are consistent with the idea that the Yellow River may be the dominant source of loess to the Loess Plateau. This would imply that dust deposition on the Loess Plateau is not only controlled by climate variations but is also controlled by the uplift and erosion of the northern Tibetan Plateau and the dynamics of large fluvial systems.

ACKNOWLEDGEMENTS

This research was funded by NERC grant NE/I008837/1 and support is gratefully acknowledged. We thank Ian Millar and Randy Parrish (NERC Isotope Science Laboratory/British Geological Survey) for helpful discussions over the manuscript.

REFERENCES

Aitchison, J., 1986. The Statistical Analysis of Compositional Data. Chapman and Hall, London.

An, Z. S., Kukla, G., Porter, S. C. & Xiao, J. L., 1991, Late Quaternary dust flow on Chinese Loess Plateau. Catena, 18, 125-132.

Andò, S., Garzanti, E., Padoan, M., Limonta, M., 2012. Corrosion of heavy minerals during weathering and diagenesis: A catalog for optical analysis. Sedimentary Geology 280, pp. 165–178

Bershaw, J., Garizone, C.N., Schoenbohm, L., Gehrels, G., Tao, L. 2012. Cenozoic evolution of the Pamir plateau based on stratigraphy, zircon provenance, and stable isotopes of foreland basin sediments at Oytag (Wuyitake) in the Tarim Basin (west China). Journal of Asian Earth Science, 44, 136-148.

Che, X. and Li, G. 2013. Binary sources of loess on the Chinese Loess Plateau revealed by U-Pb ages of zircon. Quaternary Research, 80, 545-551.

Chen, J., Li, G., Yang, J., Rao, J., Lu, H., Balsam, W., Sun, Y., Ji, J. 2007. Nd and Sr isotopic characteristics of Chinese deserts: Implications for the provenances of Asian dust. Geochim. Cosmochim. Acta, 71, 3904-3914.

Clarke, M.L., 1995, Sedimentological characteristics and rare earth element fingerprinting of Tibetan silts and their relationship with the sediments of the western Chinese Loess Plateau, *in* Derbyshire, E., ed., Wind Blown Sediments in the Quaternary Record: Chichester, UK, Quaternary Proceedings, v. 4, John Wiley and Sons, 41–51.

Derbyshire, E., Meng, X. and Kemp, R.A., 1998. Provenance, transport and characteristics of modern aeolian dust in western Gansu Province, China, and interpretation of the Quaternary loess record. J. Arid Environ., 39: 497-516.

Ding, Z.L., Derbyshire, E., Yang, S.L., Yu, Z.W., Xiong, S.F., Liu, T.S. 2002. Stacked 2.6 Ma grain size record from the Chinese loess based on five sections and correlation with the deep-sea 18O record. Paleaoceanography, 17, 1033.

Enkelmann, E., Weislogel, A., Ratschbacher, L., Eide, E., Renno, A., Wooden, J. 2007. How was the Triassic Songpan-Ganzi basin filled? A provenance study. Tectonics, 26, TC4007.

Eynaud, F., de Abreu, L., Voelker, A., Schönfeld, J., Salgueiro, E., Turon, J., Penaud, A., Toucanne, S., Naughton, F., Fernanda Sánchez Goñi, M., Malaizé, B., Cacho, I. 2007. Position of the Polar Front along the western Iberian margin during key cold episodes of the last 45 ka. Geochemistry, Geophysics, Geosystems, 10.

Formenti, P., Schutz, L., Balkanski, Y., Desboeufs, K., Elbert, M., Kandler, K., Petzold, A., Scheuvens, D., Weinbruch, S., Zhang, D. 2011. Recent progress in understanding physical and chemical properties of African and Asian mineral dust. Atmospheric Chemistry and Physics, 11, 8231-8256.

Gallet, S., Jahn, B.M. and Torii, M., 1996. Geochemical characterization of the Luochuan loess-paleosol sequence, China, and paleoclimatic implications. Chemical Geology, 133, 67-88.

Garzanti E. & Andò S. 2007. Plate tectonics and heavy-mineral suites of modern sands. In: M. Mange & D. Wright (Eds.), “Heavy Minerals in Use”, Elsevier, Amsterdam: Developments in Sedimentology Series **58**, 741-763.

Garzanti, E., Doglioni, C., Vezzoli, G., Andò, S. 2007. Orogenic belts and orogenic sediment provenance. The Journal of Geology, 115, 315-334.

Griffin, W. L., Powell, W. J., Pearson, N. J., & O'Reilly, S. Y. 2008. GLITTER: data reduction software for laser ablation ICP-MS. In P. Sylvester (Ed.), Laser Ablation-ICP-MS in the Earth Sciences: Current Practices and Outstanding Issues (Vol. 40, pp. 308–311).

Guan, Q.Y. Pan, B., Gao, H., Li, N., Zhang, H., Wang, J. 2008. Geochemical evidence of the Chinese loess provenance during the Late Pleistocene. Palaeography, Palaeoclimatology, Palaeoecology, 270, 53-58.

Guo, Z.T., Ruddiman, W.F., Hao, Q.Z., Wu, H.B., Qiao, Y.S., Zhu, R.X., Peng, S.Z., Wei, J.J., Yuan, B.Y., Liu, T.S. 2002. Onset of Asian desertification by 22 Myr ago inferred from loess deposits in China, Nature 416, 159–163.

Honda, M., Yabuki, S., and Shimizu, H., 2004, Geochemical and isotopic studies of aeolian sediments in China: Sedimentology, 51, p. 211–230.

Jackson S.E., Pearson, N.J., Griffin, W.L. & Belousova, E.A. 2004. The application of laser ablation-inductively coupled plasma-mass spectrometry to in situ U–Pb zircon geochronology. Chemical Geology 211, 47-69.

Kohfeld, K. E. and Harrison, S. P. 2003 Glacial-interglacial changes in dust deposition on the Chinese Loess Plateau. Quaternary Science Reviews, 22, 1859-1878.

Kruskal, J., 1964. Multidimensional scaling by optimizing goodness of fit to a nonmetric hypothesis. Psychometrika, 29, 1–27.

Lease, R.O., Burbank, D.W., Gehrels, G.E., Wang, Z.C. and Yuan, D.Y., 2007. Signatures of mountain building: Detrital zircon U-Pb ages from northeastern Tibet. Geology, 35, 239-242.

Li, L. and Lu, L. 2010. A preliminarily quantitative estimation of the sedimentation and erosion rates of loess deposits in the Chinese Loess Plateau over the past 250 ka. Acta Geographica Sinica, 65, 37-52.

Liou, J.G, Wang, X. & Coleman, R.G. 1989. Blueschists in major suture zones of China. Tectonics, 8, 609-619

Liu Q. S., Banerjee S. K., Jackson M. J., Chen F., Pan, Y., Zhu R., 2004: Determining the climatic boundary between the Chinese loess and paleosol: evidence from Aeolian coarse-grained magnetite. Geophysical Journal International, 156, 2, 267–274.

Liu, T.S., Ding, Z.L., 1998. Chinese loess and the palaeomonsoon, Annual Review of Earth and Planetary Science 26, 111-145.

Liu, D. 1985. Loess and the environment, China Ocean Press.

Liu, C., Masuda, A., Okada, A., Yabuki, S., and Fan, Z., 1994, Isotope geochemistry of Quaternary deposits from the arid lands in northern China: Earth and Planetary Science Letters, 127, 25–38.

Ludwig, K. R. 1999. Using Isoplot/Ex, Version 2.01: a geochronological toolkit for Microsoft Excel. In Berkeley Geochronology Center Special Publication, No. 1a (p. 47).

Lu, H.Y. and Sun, D.H., 2000. Pathways of dust input to the Chinese Loess Plateau during the last glacial and interglacial periods. Catena, 40, 251-261.

Maher, B.A., Mutch, T.J. and Cunningham, D., 2009. Magnetic and geochemical characteristics of Gobi Desert surface sediments: Implications for provenance of the Chinese Loess Plateau. Geology, 37, 279-282.

Mange, A. & Maurer, H.F.W. 1992. Heavy minerals in color. London, Chapman and Hall, 147.

Morton, A., Hallsworth, C. 2007. Stability of detrital heavy minerals during burial diagenesis. Developments in Sedimentology, 58, 215-245.

Nie, J., Horton, B.K., Saylor, J.E., Mora, A., Mange, M., Garzione, C.N., Basu, A., Moreno, C.J., Caballero, V., Parra, M. 2012. Integrated provenance analysis of a convergent retroarc foreland system: U-Pb ages, heavy minerals, Nd isotopes, and sandstone compositions of the Middle Magdalena Valley basin, northern Andes, Colombia. Earth Science Reviews, 110, 111-126.

Nie, J., Peng, W., Pfaff, K., Möller, A., Garzanti, E., Andó, S., Stevens, T., Bird, A., Chang, H., Song, Y., Liu, S., Ji, S. 2013. Controlling factors on heavy mineral assemblages in Chinese loess and Red Clay. Palaeogeography, Palaeoclimatology, Palaeoecology, 381-382, 110-118.

Nie, J., Song, Y., Möller, A., Stockli, D.F., Peng, W., Stevens, T., Bird, A., Oalmann, J., Liu, S., Horton, B.K., Fang, X., 2014. Provenance of the upper Miocene-Pliocene Red Clay deposits of the Chinese Loess Plateau. Earth and Planetary Science Letters, 407, 35-47.

Philip, G. 1968. Mineralogy of recent sediments of Tigris and Euphrates rivers and some older detritial deposits. Journal of Sedimentary Petrology, 38, 35-44.

Pullen, A., Kapp, P., McCallister, A.T., Chang, H., Gehrels, G.E., Garzione, C.N., Heermance, R.V., Ding, L. 2011. Qaidam Basin and northern Tibetan Plateau as dust sources for the Chinese Loess Plateau and paleoclimatic implications. Geology, 39, 1031-1034.

Pye, K., and Zhou, L.P., 1989, Late Pleistocene and Holocene aeolian dust deposition in North China and the Northwest Pacifi c Ocean: Paleogeography, Paleoclimatology, Paleoecology, v. 73, p. 11–23.

Qiang, X., An, Z., Song, Y., Chang, H., Sun, Y., Liu, W., Ao, H., Dong, J., Fu, C., Wu, F., Cai, W., Cao, J., Xu, X., Ai, L. 2011. New eolian red clay sequence on the western Chinese Loess Plateau linked to onset of Asian desertification about 25 Ma ago. Science China Earth Sciences, 54, 136-144.

Roe, G. 2009. On the interpretation of Chinese loess as a paleoclimate indicator. Quaternary Research, 71, 150-161.

Slama, J., Kosler, J. 2012. Effects of sampling and mineral separation on accuracy of detrital zircon studies. Geochemistry, Geophysics, Geosystems, 13, 1525-2027.

Stevens, T., Palk, C., Carter, A., Lu, H. and Clift, P.D., 2010. Assessing the provenance of loess and desert sediments in northern China using U-Pb dating and morphology of detrital zircons. Geol. Soc. American Bulletin, 122: 1331-1344.

Stevens, T., Adamiec, G., Bird, A., Lu, H. 2013a. An abrupt shift in dust source on the Chinese Loess Plateau revealed through high sampling resolution OSL dating. Quaternary Science Reviews, 82.

Stevens, T. Carter, A., Watson, T., Vermeesch, P., Andò, S., Bird, A., Lu, H., Garzanti, E., Cottam, M., Sevastjanova, I. 2013b. Genetic linkage between the Yellow River, the Mu Us desert, and the ChineseLoess Plateau. Quaternary Science Reviews, 78, 355-368.

Sun J., Liu T., 2000. Multiple origins and interpretations of the magnetic susceptibility signal in Chinese wind-blown sediments. Earth and Planetary Science Letters, 180, 287–296.

Sun, J.M. 2000. Origin of eolian sand mobilization during the past 2300 years in the Mu Us desert, China. Quaternary Research, 53, 78-88.

Sun, J., 2002, Provenance of loess material and formation of loess deposits on the Chinese Loess Plateau: Earth and Planetary Science Letters, 203, 845–859.

Sun, J., 2005, Nd and Sr isotopic variations in Chinese eolian deposits during the past 8 Ma: Implications for provenance change: Earth and Planetary Science Letters, v. 240, p. 454–466, doi: 10.1016/j.epsl.2005.09.019.

Sun, J., Ye, J., Wu, W., Ni, X., Bi, S., Liu, W., Meng, J. 2010. Late Oligocene-Miocene mid-latitude aridification and wind patterns in the Asian interior. Geology, 38, 515-518.

Sun, Y., Tada, R., Chen, J., Liu, Q., Toyoda, S., Tani, A., Ji, J., Isozaki, Y., 2008, Tracing the provenance of fine-grained dust deposited on the central Chinese Loess Plateau: Geophysical Research Letters, 35, p. L01804.

Sun, J., Zhu, X. 2010. Temporal variations in Pb isotopes and trace element concentrations within Chinese eolian deposits during the past 8 Ma: Implications for provenance change. Earth and Planetary Science Letters, 290, 438-447

Vermeesch, P., 2004, How many grains are needed for a provenance study? Earth and Planetary Science Letters, 224, 3-4, 441-45.

Vermeesch, P., 2012. On the visualisation of detrital age distributions. Chemical Geology, 312: 190-194.

Vermeesch, P., 2013. Multi-sample comparison of detrital age distributions. Chem. Geol., 341(0): 140-146.

Wang, Y.J., Cheng, H., Edwards, R.L., An, Z.S., Wu, J.Y., Sen, C.-C. & Dorale, J.A. 2001. A High-Resolution Absolute-Dated Late Pleistocene Monsoon record from Hulu Cave, China. Science, 294, 2345-2348.

Wang, P.X., Clemens, S., Beaufort, L., Braconnot, P., Ganssen, G., Jian, Z., Peter Kershaw, P., Sarnthein, M., 2005. Evolution and variability of the Asian monsoon system: state of the art and outstanding issues. Quaternary Science Reviews, 24, 595-629.

Wang, Y.X., Yang, J.D., Chen, J., Zhang, K.J., Rao, W.B. 2007. The Sr and Nd isotopic variations of the Chinese Loess Plateau during the past 7 Ma: Implications for the East Asian winter monsoon and source areas of loess. Paleogeography, Paleoclimatology, Paleoecology, 249, 351-361.

Wu, G., Zhang, C., Gao, S., Yao, T., Tian, L., and Xia, D., 2009, Element composition of dust from a shallow Dunde ice core, Northern China: Global and Planetary Change, 67, 186–192.

Xiao, G., Zong, K., Li, G., Hu, Z., Dupont-Nivet, G., Peng, S. & Zhang, K. 2012. Spatial and glacial-interglacial variations in provenance of the Chinese Loess Plateau. Geophys. Res. Lett., 39(20): L20715.

Xie, J., Wu, F.Y. and Ding, Z.L., 2007. Detrital zircon composition of U-Pb ages and Hf isotope of the Hunshandake sandland and implications for its provenance. Acta Petrol. Sin., 23, 523-528.

Yang, S., Ding, Z. 2010. Drastic climatic shift at ~2.8 Ma as recorded in eolian deposits of China and its implications for redefining the Pliocene-Pleistocene boundary. Quaternary International, 219, 37-44.

Zhao, W., Sun, Y., Balsam, W., Lu, H., Liu, L., Chen, J., Ji, J. 2014, Hf-Nd isotopic variability in mineral dust from Chinese and Mongolian deserts: implications for sources and dispersal. Scientific Reports, 4, 5837.

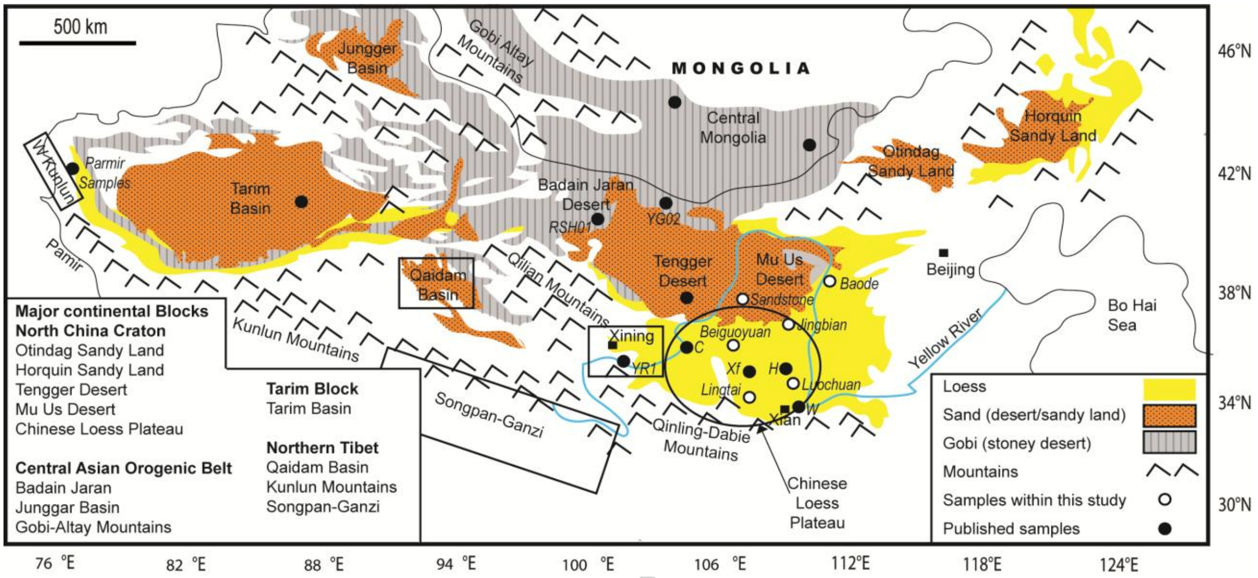
500 km
MONGOLIA
Jungger Basin
Gobi Altay Mountains
Central Mongolia
Otindag Sandy Land
Horquin Sandy Land
W-Kunlun
Parmir Samples
Pamir
Tarim Basin
Badain Jaran Desert
YG02
RSH01
Qaidam Basin
Qilian Mountains
Tengger Desert
Mu Us Desert
Sandstone
Baode
Beijing
Bo Hai Sea
Yellow River
Jingbian
Beiguoyuan
Xining
C
YR1
Xf
H
Luochuan
Lingtai
W
Xian
Kunlun Mountains
Songpan-Ganzi
Qinling-Dabie Mountains
Chinese Loess Plateau
Major continental Blocks
North China Craton
Otindag Sandy Land
Horquin Sandy Land
Tengger Desert
Mu Us Desert
Chinese Loess Plateau
Central Asian Orogenic Belt
Badain Jaran
Junggar Basin
Gobi-Altay Mountains
Tarim Block
Tarim Basin
Northern Tibet
Qaidam Basin
Kunlun Mountains
Songpan-Ganzi
Loess
Sand (desert/sandy land)
Gobi (stoney desert)
Mountains
Samples within this study
Published samples
46°N
42°N
38°N
34°N
30°N
76 °E
82 °E
88 °E
94 °E
100 °E
106 °E
112°E
118°E
124°E

Figure 1

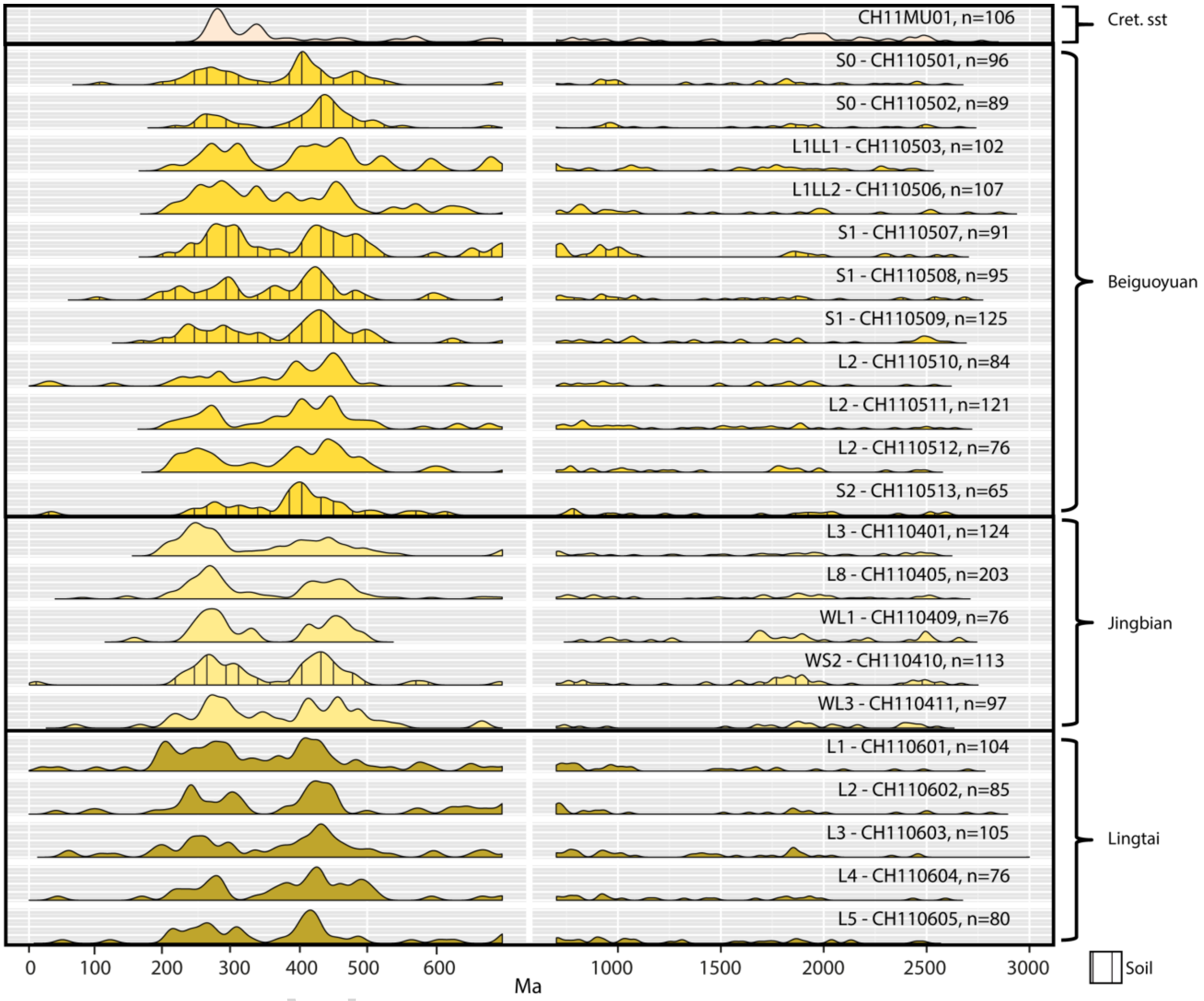
CH11MU01, n=106
Cret. sst
S0 - CH110501, n=96
S0 - CH110502, n=89
L1LL1 - CH110503, n=102
L1LL2 - CH110506, n=107
S1 - CH110507, n=91
S1 - CH110508, n=95
S1 - CH110509, n=125
L2 - CH110510, n=84
L2 - CH110511, n=121
L2 - CH110512, n=76
S2 - CH110513, n=65
Beiguoyuan
L3 - CH110401, n=124
L8 - CH110405, n=203
WL1 - CH110409, n=76
WS2 - CH110410, n=113
WL3 - CH110411, n=97
Jingbian
L1 - CH110601, n=104
L2 - CH110602, n=85
L3 - CH110603, n=105
L4 - CH110604, n=76
L5 - CH110605, n=80
Lingtai
0
100
200
300
400
500
600
1000
1500
2000
2500
3000
Ma
Soil

Figure 2

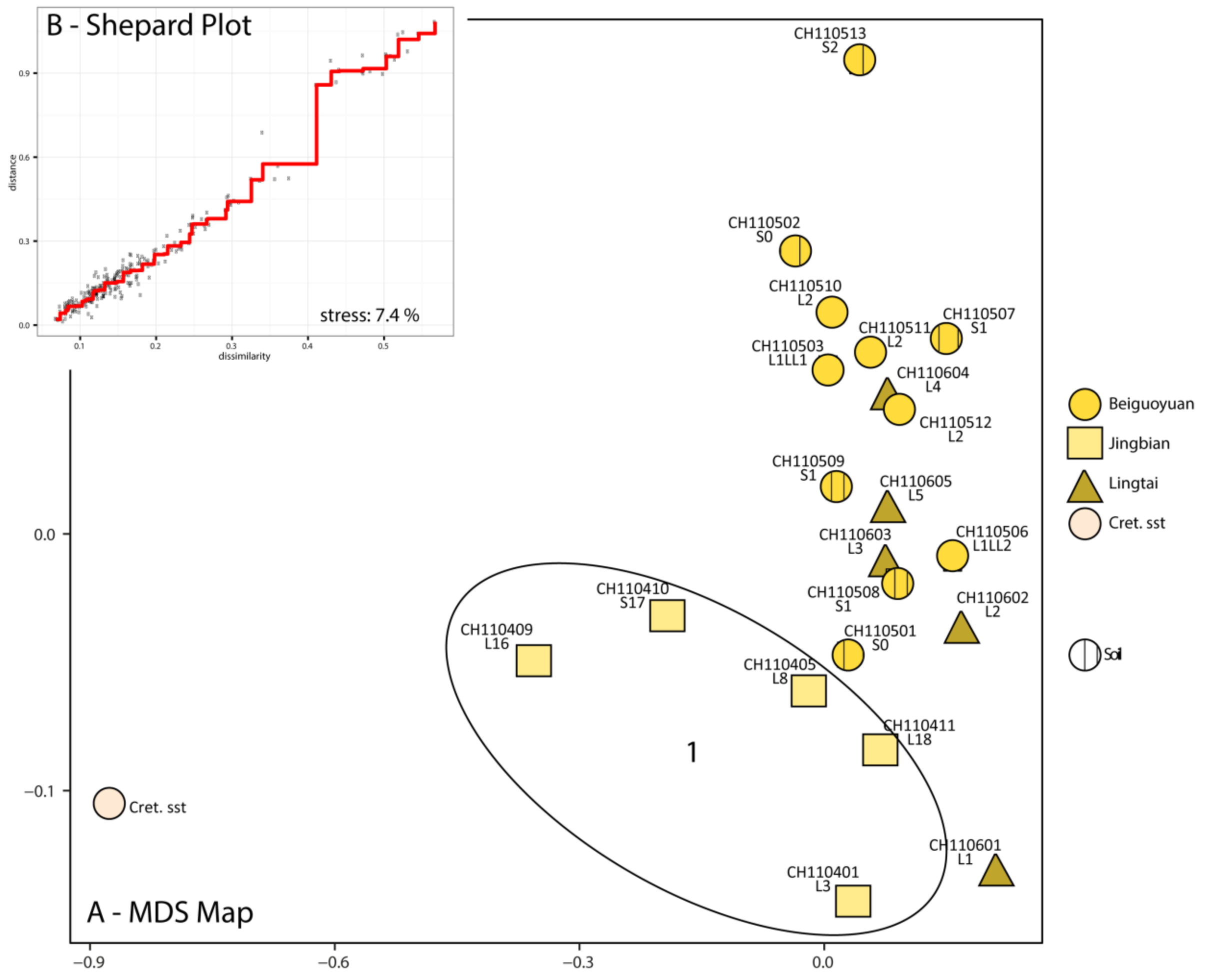
B - Shepard Plot
0.9
0.6
0.3
0.0
distance
0.1
0.2
0.3
0.4
0.5
dissimilarity
stress: 7.4 %
CH110513
S2
CH110502
S0
CH110510
L2
CH110507
S1
CH110511
L2
CH110503
L1LL1
CH110604
L4
CH110512
L2
CH110509
S1
CH110605
L5
CH110603
L3
CH110506
L1LL2
CH110410
S17
CH110508
S1
CH110602
L2
CH110409
L16
CH110501
S0
CH110405
L8
CH110411
L18
1
Cret. sst
CH110601
L1
CH110401
L3
A - MDS Map
0.0
−0.1
−0.9
−0.6
−0.3
0.0
Beiguoyuan
Jingbian
Lingtai
Cret. sst
Soil

Figure 3

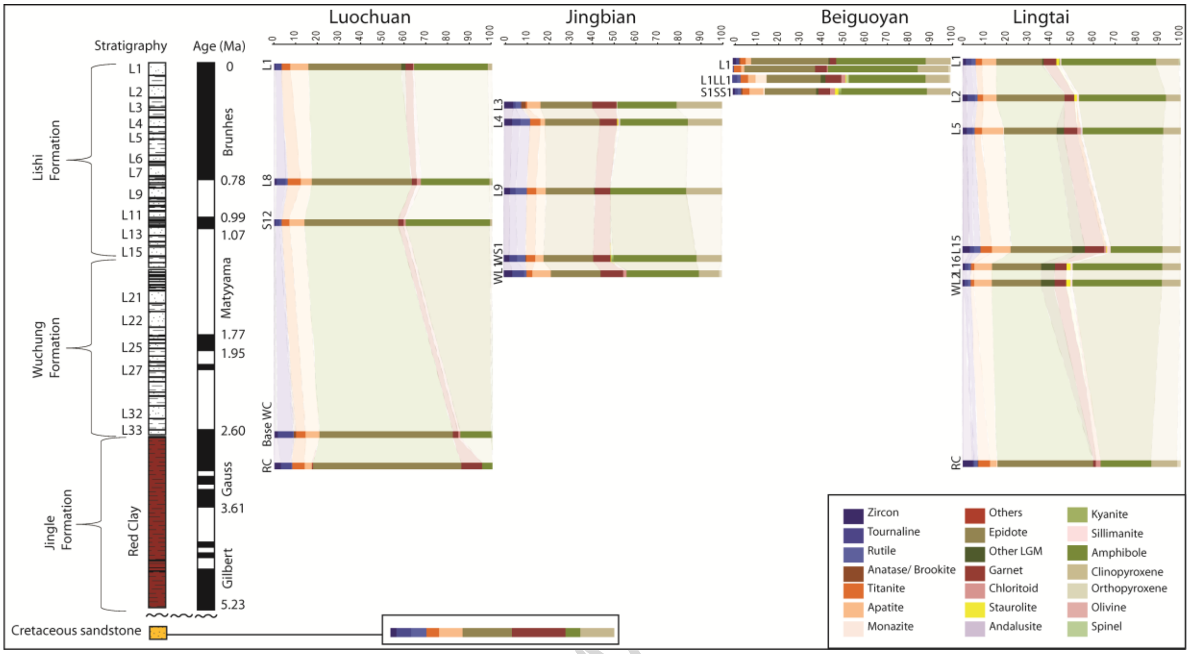
Luochuan
Jingbian
Beiguoyan
Lingtai
Stratigraphy
Age (Ma)
Lishi Formation
Wuchung Formation
Jingle Formation
Red Clay
Cretaceous sandstone
L1
L2
L3
L4
L5
L6
L7
L9
L11
L13
L15
L21
L22
L25
L27
L32
L33
0
0.78
0.99
1.07
1.77
1.95
2.60
3.61
5.23
Brunhes
Matyyama
Gauss
Gilbert
S12
L8
Base WC
RC
L3
L4
L9
WL WS1
L1
L1LL1
S1SS1
L2
L5
L15
L16
WL2
0
10
20
30
40
50
60
70
80
90
100
Zircon
Tournaline
Rutile
Anatase/ Brookite
Titanite
Apatite
Monazite
Others
Epidote
Other LGM
Garnet
Chloritoid
Staurolite
Andalusite
Kyanite
Sillimanite
Amphibole
Clinopyroxene
Orthopyroxene
Olivine
Spinel

Figure 4

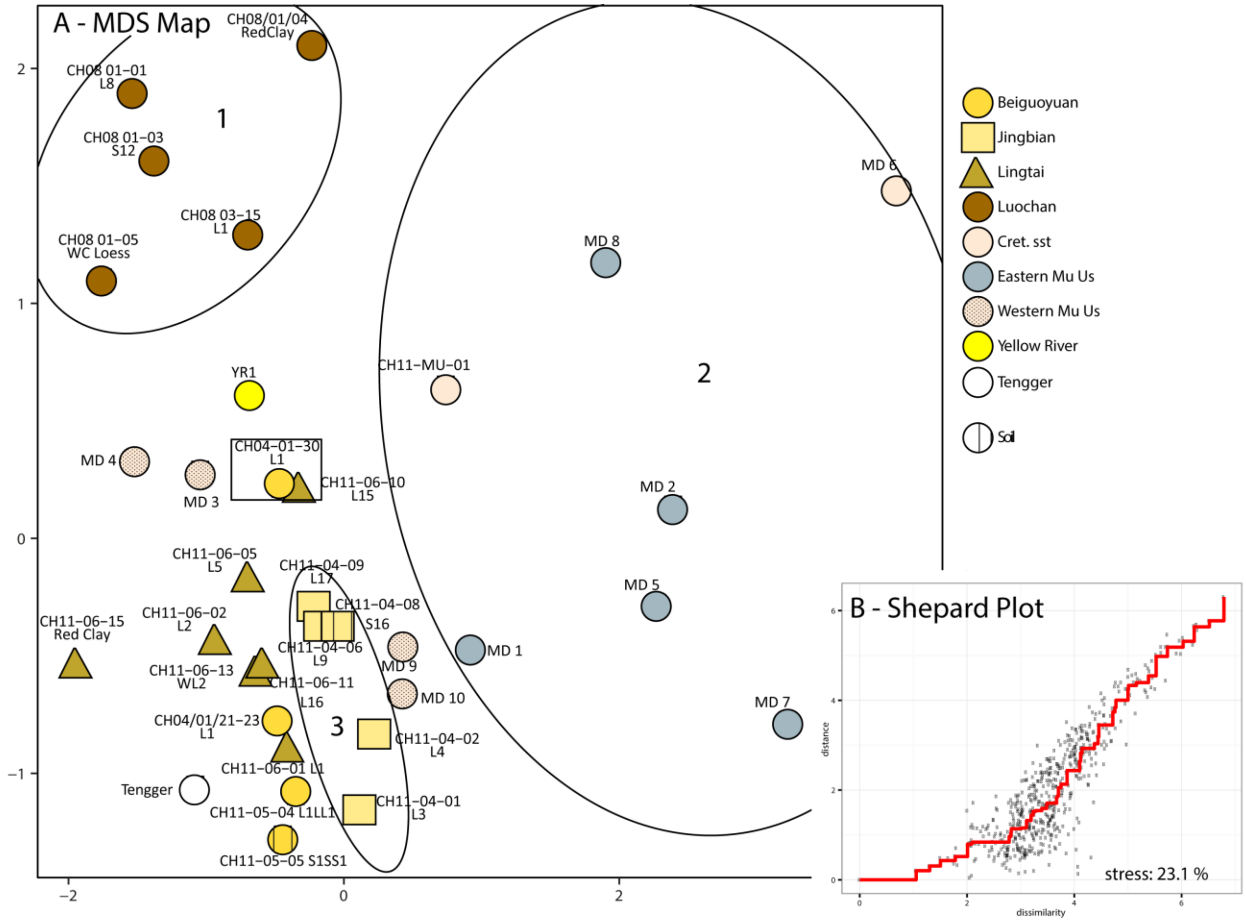
A - MDS Map
CH08/01/04 RedClay
CH08 01–01 L8
1
CH08 01–03 S12
CH08 03–15 L1
CH08 01–05 WC Loess
YR1
CH11–MU–01
2
MD 6
MD 8
MD 4
MD 3
CH04–01–30 L1
CH11–06–10 L15
MD 2
CH11–06–05 L5
CH11–04–09 L17
CH11–04–08 S16
CH11–06–15 Red Clay
CH11–06–02 L2
CH11–04–06 L9
MD 9
MD 1
MD 5
CH11–06–13 WL2
CH11–06–11 L16
MD 10
CH04/01/21–23 L1
3
CH11–04–02 L4
MD 7
CH11–06–01 L1
Tengger
CH11–05–04 L1LL1
CH11–04–01 L3
CH11–05–05 S1SS1
2
1
0
−1
−2
0
2
Beiguoyuan
Jingbian
Lingtai
Luochan
Cret. sst
Eastern Mu Us
Western Mu Us
Yellow River
Tengger
Soil
B - Shepard Plot
distance
dissimilarity
0
2
4
6
stress: 23.1 %

Figure 5

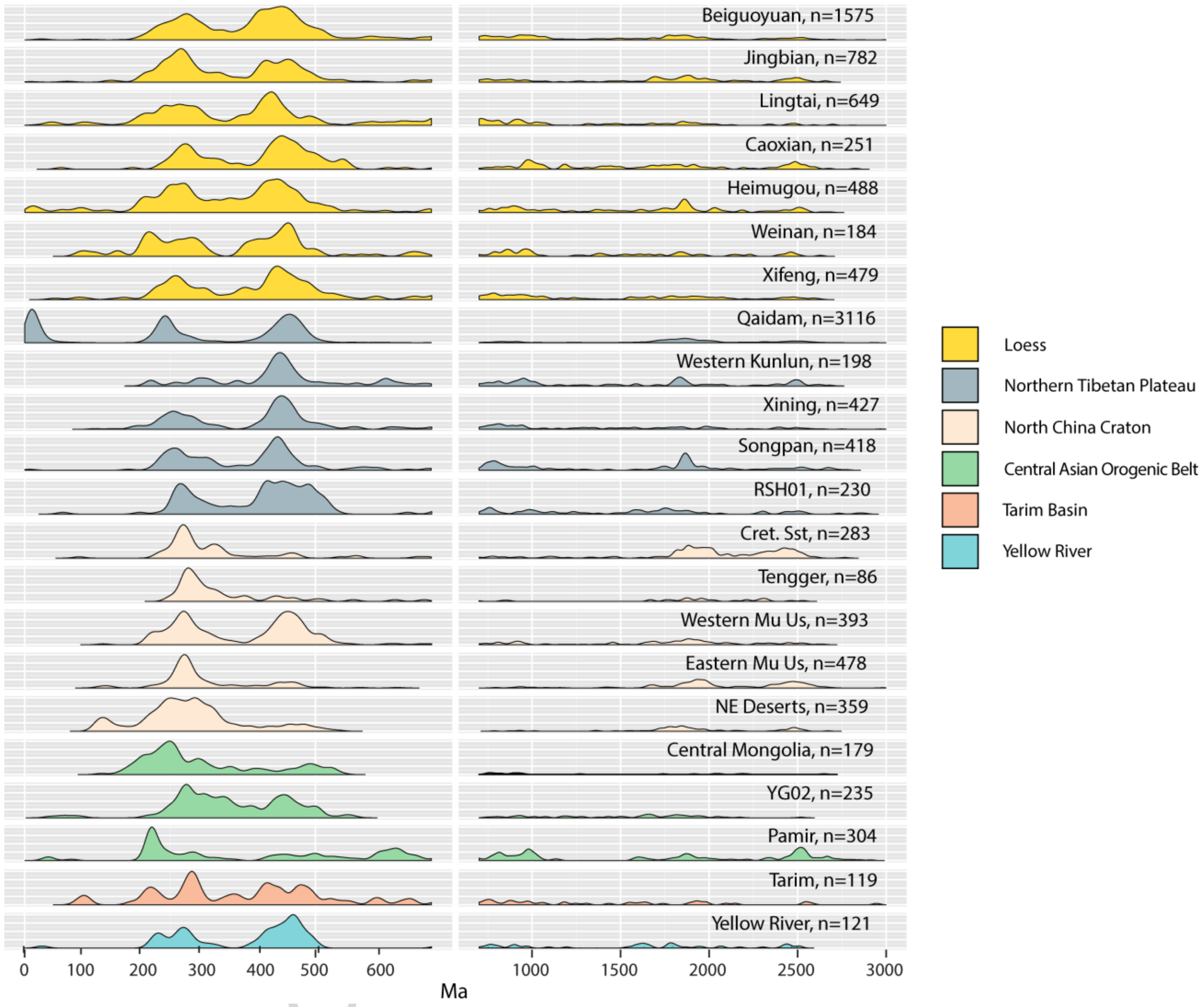
Beiguoyuan, n=1575
Jingbian, n=782
Lingtai, n=649
Caoxian, n=251
Heimugou, n=488
Weinan, n=184
Xifeng, n=479
Qaidam, n=3116
Western Kunlun, n=198
Xining, n=427
Songpan, n=418
RSH01, n=230
Cret. Sst, n=283
Tengger, n=86
Western Mu Us, n=393
Eastern Mu Us, n=478
NE Deserts, n=359
Central Mongolia, n=179
YG02, n=235
Pamir, n=304
Tarim, n=119
Yellow River, n=121
0
100
200
300
400
500
600
1000
1500
2000
2500
3000
Ma
Loess
Northern Tibetan Plateau
North China Craton
Central Asian Orogenic Belt
Tarim Basin
Yellow River

Figure 6

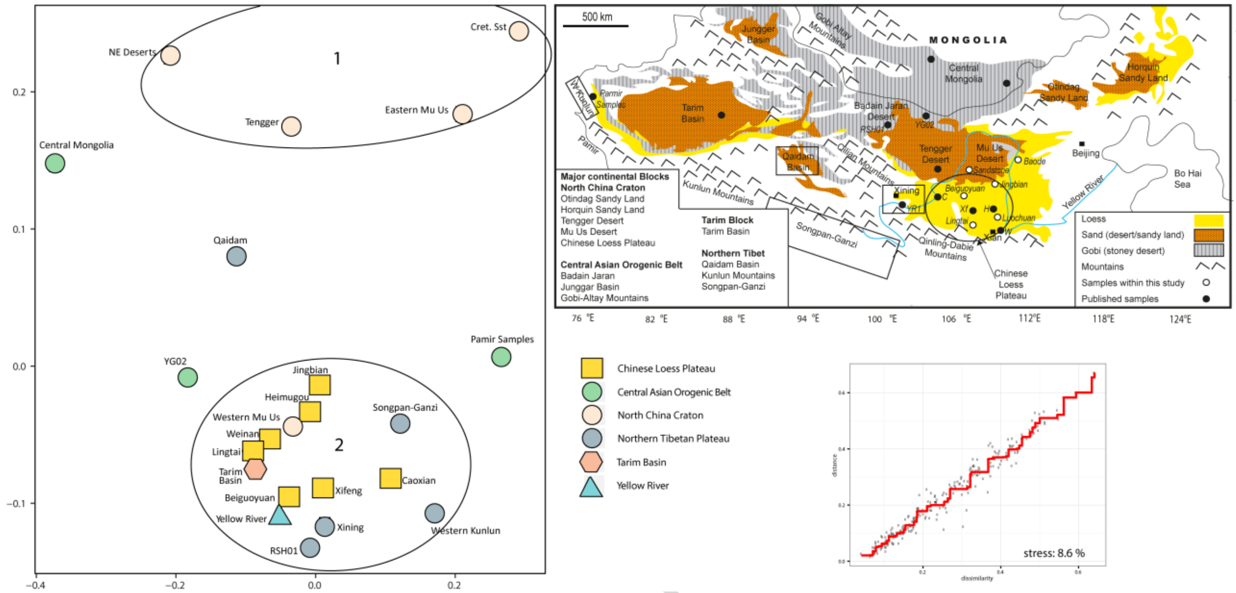

Cret. Sst
NE Deserts
1
Tengger
Eastern Mu Us
Central Mongolia
Qaidam
Pamir Samples
YG02
Jingbian
Heimugou
Songpan-Ganzi
Western Mu Us
Weinan
Lingtai
2
Tarim Basin
Caoxian
Xifeng
Beiguoyuan
Yellow River
Xining
Western Kunlun
RSH01
0.2
0.1
0.0
−0.1
−0.4
−0.2
0.0
0.2
500 km
Jungger Basin
Gobi Altay Mountains
MONGOLIA
Central Mongolia
Horquin Sandy Land
Otindag Sandy Land
W-Kunlun
Parmir Samples
Tarim Basin
Badain Jaran Desert
RSH01
YG02
Pamir
Qaidam Basin
Qilian Mountains
Tengger Desert
Mu Us Desert
Baode
Sandstone
Beijing
Bo Hai Sea
Yellow River
Jingbian
Beiguoyuan
Xining
C
YRT
Xf
H
Luochuan
Lingtai
W
Xian
Kunlun Mountains
Songpan-Ganzi
Qinling-Dabie Mountains
Chinese Loess Plateau
Major continental Blocks
North China Craton
Otindag Sandy Land
Horquin Sandy Land
Tengger Desert
Mu Us Desert
Chinese Loess Plateau
Central Asian Orogenic Belt
Badain Jaran
Junggar Basin
Gobi-Altay Mountains
Tarim Block
Tarim Basin
Northern Tibet
Qaidam Basin
Kunlun Mountains
Songpan-Ganzi
Loess
Sand (desert/sandy land)
Gobi (stoney desert)
Mountains
Samples within this study
Published samples
46°N
42°N
38°N
34°N
30°N
76 °E
82 °E
88 °E
94 °E
100 °E
106 °E
112°E
118°E
124°E
Chinese Loess Plateau
Central Asian Orogenic Belt
North China Craton
Northern Tibetan Plateau
Tarim Basin
Yellow River
distance
0.0
0.2
0.4
0.6
dissimilarity
0.2
0.4
0.6
stress: 8.6 %

Figure 7

Sample	unit	Lithology	Heavy Mineral count	Zircon U-Pb data
Luochuan - N35 43.613' E109 25.809'				
CH08/03/15-U-Pb	L1	Loess	X	
CH08/01/01-U-Pb	L8	Loess	X	
CH08/01/03-U-Pb	S12	Soil	X	
CH08/01/04-U-Pb	red clay	Clay	X	
CH08/01/05-U-Pb	base L34		X	
Jingbian - N37 29.923 E108 54.281				
CH11-04-01	L3	Loess	X	X
CH11-04-02	L4	Loess	X	
CH11-04-05	L8	Loess		X
CH11-04-06	L9	Loess	X	
CH11-04-08	S16	Soil	X	
CH11-04-09	L16	Loess	X	X
CH11-04-10	S17	Soil		X
CH11-04-11	L18	Loess		X
Beiguoyuan - N36 37.355' E107 17.203'				
CH11-05-01	S0 Upper	Soil		X
CH11-05-02	S0 Middle	Soil		X
CH11-05-03	L1LL1	Loess		X
CH04/01/21-23	L1		X	
CH04-01-30	L1		X	
CH11-05-04	L1LL1		X	
CH11-05-05	S1SS1	Soil	X	
CH11-05-06	L1LL2	Loess		X
CH11-05-07	S1	Soil		X
CH11-05-08	S1	Soil		X
CH11-05-09	S1	Soil		X
CH11-05-10	L2	Loess		X
CH11-05-11	L2	Loess		X
CH11-05-12	L2	Loess		X
CH11-05-13	S2	Soil		X
Lingtai - N34 59.242 E107 33.134				
CH11-06-01	L1	Loess	X	X
CH11-06-02	L2	Loess	X	X
CH11-06-03	L3	Loess		X
CH11-06-04	L4	Loess		X
CH11-06-05	L5	Loess	X	X
CH11-06-10	L15	Loess	X	
CH11-06-11	L16	Loess	X	
CH11-06-13	WL2	Loess	X	
CH11-06-15	RC	Clay	X	
Cretaceous Sandstone				
CH11-MU-01	Cretaceous Sandstone	Sandstone	X	X

Table 1.

FIGURE CAPTIONS

Figure 1. Map of China adapted from Xiao et al. (2012) and Nie et al. (2014). Samples/sections analyzed within this study are marked by circles with a white fill. Samples previously analyzed are marked by filled black circles. Some previously published samples are individually named as they are referred to within the text, C – Caoxian; H – Heimugou (Pullen et al., 2011); W – Weinan; Xf – Xifeng (Xie et al., (201); RSH01 and YG02 (Che and Li 2013); YR1 – (Stevens et al., 2013b), Parmir samples – (Bershaw et al., 2012). Individual locations of samples from the Qaidam Basin (Lease et al., 2007; 2012; Pullen et al., 2011), the Mu Us Desert (Stevens et al., 2010; 2013b), Songpan-Ganzi (Enkelmann et al., 2007; Pullen et al., 2011), western Kunlun (W Kunlun) (Bershaw et al., 2012) and Xining (Xiao et al., 2012 and Lease et al., 2007) are not shown due to space limitations. Samples in central Mongolia and Tarim are from Xie et al. (2007).

Figure 2. KDEs for samples with zircon U-Pb data analyzed within this study. The KDEs are split at 700 Ma to enlarge the period between 0-700 Ma, where distinctive peaks are seen. The bandwidth used is 20 Ma. Each loess/soil section has been given a different colour and the soils are highlighted with vertical lines within the shaded area of the age spectra.

Figure 3. A - MDS map of zircon U-Pb analyses within this study. A circle has been drawn around the group of data point from Jingbian to highlight their close relationship and has been numbered to help discussion. Axes are in KeS units' (0<KS<1) of distance between the samples (Vermeesch 2013). B – Shepard plot giving the stress value of the fit of the 'goodness of fit' of the MDS map. The stress value is low suggesting a very good fit of the data.

Figure 4. Heavy mineral counts against stratigraphic position and age. Other LGM – other low grade metamorphic minerals, e.g. clinozoisite, allanite, zoisite, prehnite and pumpellyite. The shaded areas

between the samples are there to highlight variations between the samples down-section and not an interpretation of the rate at which the mineral counts vary between samples.

Figure 5. A - MDS map of heavy mineral analyses within this study compared to samples from Stevens et al. (2013a; b) from the Mu Us Desert (MD), Tengger Desert (TD), Yellow River (YR) and Beiguoyuan. Circles have been drawn around groupings of points and have been numbered to help discussion. Axes are in KeS units' (0<KS<1) of distance between the samples (Vermeesch 2013). B – Shepard plot giving the stress value of the fit of the 'goodness of fit' of the MDS map, the stress value is higher here (23.1%), suggesting a weaker fit of the MDS map.

Figure 6. KDEs for samples with zircon U-Pb data analyzed within this study and previously published data from Bershaw et al. (2012), Che and Li (2013), Enkelmann et al. (2007), Lease et al. (2007;2012), Pullen et al. (2011), Stevens et al. (2010, 2013b), Xiao et al. (2012) and Xie et al. 2007. The KDEs are split at 700 Ma to enlarge the period between 0-700 Ma, where distinctive peaks are seen. The bandwidth used is 20 Ma.

Figure 7. A - MDS map of zircon U-Pb data from this study compared to previously published work from Bershaw et al. (2012), Che and Li (2013), Enkelmann et al. (2007), Lease et al. (2007;2012), Pullen et al. (2011), Stevens et al. (2010, 2013b), Xiao et al. (2012) and Xie et al. 2007. Axes are in KeS units' (0<KS<1) of distance between the samples (Vermeesch 2013). Circles have been drawn around data points that are similar and numbered to aid discussion. B – Shepard plot giving the stress value of the fit of the 'goodness of fit' of the MDS map, it has a low stress value, suggesting the fit is good.

TABLE CAPTIONS

Table 1. Details of samples analyzed within this study and the different methods applied to these samples.

Highlights

Largest single grain provenance dataset yet assembled for Quaternary Chinese Loess

First systematic combined zircon U-Pb age and heavy mineral approach on loess

North Tibetan dust source dominates but some spatial variation across Loess Plateau

No consistent changes in loess provenance between glacial and interglacial periods